

## RESEARCH ARTICLE

# ENHANCED AVO USING LAMÉ PETROPHYSICAL FLUID STACKS PARAMETERS FOR GAS DETECTION IN SANDSTONE OVER AN X FIELD, NIGERIAN NIGER DELTA

Ohakwere-Eze M.C.

Geophysics Research Group, Department of Physics, Federal University of Kashere, Gombe State.

\*Corresponding Author Email: [michael.ohakwereze@gmail.com](mailto:michael.ohakwereze@gmail.com)

This is an open access journal distributed under the Creative Commons Attribution License CC BY 4.0, which permits unrestricted use, distribution, and reproduction in any medium, provided the original work is properly cited.

## ARTICLE DETAILS

## Article History:

Received 01 January 2023  
Revised 03 February 2023  
Accepted 07 March 2023  
Available online 13 March 2023

## ABSTRACT

Here we demonstrate the separation of gas sand from surrounding shale using Lamé petrophysical parameters;  $\lambda$ ,  $\mu$  and  $\frac{\lambda}{\mu}$  where other rock attribute fails to give such clear distinction. Gather stacks (near and far) were generated to improve fidelity of pre-stack seismic. AVO models were generated then combined and inverted with the Seismic gathers to generate Impedance volumes ( $Z_p$  and  $Z_s$ ) which were transformed to volumes of the Lamé attributes. Results of this method on the logs and pre-stack seismic gathers show significant improvement in DHI detectability over the conventional analysis based on  $V_p/V_s$  or  $Z_p$ ,  $Z_s$ , variations. The results show that moderate to high values of  $\mu$  were indicative of clean sands and lower values of  $\lambda$  and  $\frac{\lambda}{\mu}$  ( $<1$ ) are indicative of high porosity and therefore high reserves in place, in this case gas.

The good correlation of the results of the  $\lambda$  and  $\frac{\lambda}{\mu}$  inversion volumes with those of rock physics analysis observed at the well provided confidence in our interpretation of a prospect away from the well thereby leading to discovery of another potential field in the region.

## KEYWORDS

AVO/AVA, gas detection, seismic inversion, DHI, Lamé's parameters.

## 1. INTRODUCTION

Several notable authors have used traditional AVO and petrophysical analysis to identify and analyze anomalous variations between seismic compressional wave velocity ( $V_p$ ) and shear wave velocity ( $V_s$ ) for the purpose to map out changes primarily in pore fluid as well as lithologic properties (Gassmann, 1951; Castagna, 1993a). Other have used other analysis methods using Poisson's ratio,  $\sigma$  (Ostrander 1984) or P and S reflectivities, from which impedance contrast is derived (Ekwe et al., 2012; Fatti et al., 1994). Reservoir characterization is one of the most important components of seismic data interpretation. Conventional practice was to delineate the reservoir using post-stack seismic data while prestack seismic data was completely ignored.

Velocity measurements can be converted to Lamé moduli parameters of rigidity ( $\lambda$ ) and incompressibility ( $\mu$ ) which gives new insight into the original governing rock property factor. Note that anomalous points in the  $R_p$ ,  $R_s$  crossplot do not necessarily translate into a hydrocarbon filled zone. There are many lithologic/fluid combinations that can produce AVO anomalies and care should be taken in interpreting the results. That being said, obvious AVO anomalies are a step in the right direction to identifying potential hydrocarbon reservoirs (Perez, et al., 2010). At the early stage of AVO technology, bright spot, phase reversal, and dim out anomalies were largely used to recognize hydrocarbon anomalies on stacked seismic profiles. However, all bright anomalies may not be due to hydrocarbons and may need proper validation before drilling (Nanda, 2016).

The research aim is to use rock Physics analysis of well log data and attributes from AVO inversion of the anisotropic 3D Seismic data to delineate the lithology and fluid property moreover to evaluate these

properties. Thus, integration of these seismic tools proves to be a robust methodology for discerning fluids and lithology since it provides geological information, which helps to propose new well locations. Integrating rock physics and seismic data inversion will help to identify bypassed hydrocarbon bearing sands in parts of an old oil field, away from existing wells so as to create new exploration and development opportunities in the field. The main contribution of this research work is therefore to show that bypassed reservoirs could still be recovered from matured oilfields using the approach proposed leading to optimized volumetrics. The reasons for focusing on gas-sand reflections is that the attributes contrast between a gas sand and the encasing medium is usually large, meaning that gas sands have detectable changes in amplitude with offset.

2. THEORY OF THE LAMBDA-MU-RHO ( $\lambda$ - $\mu$ - $\rho$ ) METHOD

Recall the underlying physics equations for the P-wave velocity,  $V_p$  and S-wave velocity expressed as follows:

$$V_p = \sqrt{\frac{\lambda + 2\mu}{\rho}} \quad (1)$$

$$V_s = \sqrt{\frac{\mu}{\rho}} \quad (2)$$

$\lambda$  (Pronounced Lamda) is the first Lamé constant (incompressibility) related to pore fluid.

$\mu$  (pronounced rho) is the second Lamé constant (shear modulus or rigidity) related to the rock matrix.

## Quick Response Code



## Access this article online

Website:  
[www.actachemicamalaysia.com](http://www.actachemicamalaysia.com)

DOI:  
10.26480/acmy.01.2023.35.40

Castagna, have given an empirical linear transform equation that shows the relationship between  $V_p$  and  $V_s$ , given  $c_1$  and  $c_2$  as empirical regression coefficients shown below (Castagna, 1985).

$$V_s = c_1.V_p + c_2$$

Also, given the P-impedance,  $Z_p$  and S-impedance,  $Z_s$  equations as follows.

$$Z_p = V_p.\rho = \sqrt{(\lambda + 2\mu)\rho} \quad (3)$$

$$Z_s = V_s.\rho = \sqrt{\mu\rho} \quad (4)$$

Where  $\rho$  (pronounced rho) is the density.

The proposal here is to extract the the moduli terms,  $\lambda$  and  $\mu$  from the moduli /density relationships to velocities  $V$  or impedances  $Z$ , as expressed in equations 3 and 4.

From these relationships we can extract the orthogonal Lamé parameters from logs with measured density or  $\lambda\mu\rho$  volume (i.e.  $\lambda\rho$ ,  $\mu\rho$ ) from seismic without known density. The equations are thus;

$$\lambda = V_p^2.\rho - 2V_s^2.\rho \quad (5)$$

$$\mu = V_s^2.\rho \quad (6)$$

$$\lambda\rho = Z_p^2 - 2Z_s^2 \quad (7)$$

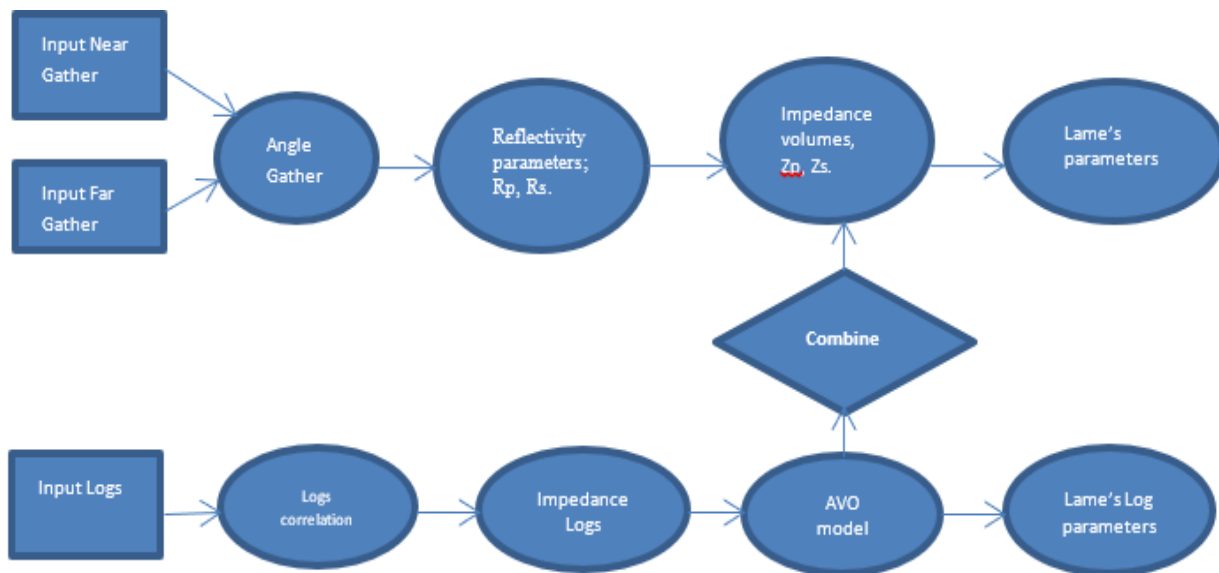


Figure 1: Flow chat illustrating methodology.

Shear wave logs were generated empirically according to Castagna's linear transform equation. Fluid substitution was performed to verify and obtain correct log values over the gas sand interval. After necessary log corrections and correlation, different attributes including various combined transforms of the Lamé parameters were generated ( $V_p/V_s$ ,  $V_p/V_s^2$ ,  $\lambda+2\mu$ ,  $\lambda$ ,  $\mu$ ,  $\frac{\lambda}{\mu}$  etc). They were then analyzed for sensitivity to both lithology and fluids. Crossplots of the attributes from logs ( $I_p$ ,  $I_s$ ,  $\lambda\rho$ ,  $\mu\rho$  and  $\frac{\lambda}{\mu}$ ) were generated. The well log analysis method employed is efficient and less expensive in prospecting for hydrocarbons and is reliable when combined with other geophysical methods such as seismic and core analysis (Ohakwere-Eze et al., 2018). Gather stacks (near and far) were generated to improve fidelity of pre-stack seismic. AVO models were generated then combined and inverted with the Seismic gathers to generate Impedance volumes ( $Z_p$  and  $Z_s$ ) which were transformed to volumes of the Lamé attributes. These volumes were studied around the well location to validate the known prospect while looking away from the well for possible prospect(s).

#### 4. RESULTS AND DISCUSSION

Figure 2 shows logs in depth from the study area where a conventional analysis of the  $Z_p$  and  $Z_s$  logs (track 1 and 2 respectively) has limitations in clearly discriminating between all the various lithology and gas sand zones. By contrast the  $\lambda\rho$  log (track 3) shows a sharp deflection to the left on entering the gas sand zone and deflects sharply to the far right on leaving that zone which is an excellent indicator of a capping shale.

$$\mu\rho = Z_s^2 \quad (8)$$

Goodway, and Dewar and Downton established seismic reservoir characterization using Lamé parameters (Goodway, 1999; 2001; Dewar and Downton, 2002). The ratio between incompressibility ( $\lambda$ ) and rigidity ( $\mu$ ) i.e  $\lambda/\mu$  is the basic principle for mapping lithology where ratios less than 1 are highlighted as sand zones. The incompressibility parameter  $\lambda$  is the only Lamé parameter that serves as a fluid discriminator assuming the rock properties do not change. Assuming it is sand, the pores can be filled with a variety of fluids which the lesser the density will reduce the incompressibility, brine being the least while gas the most.

Some group researchers gave a modified equation from the Knott-Zoeppritz equations to extract P and S reflectivities or impedance contrasts given as (Gidlow et al., 1992; Fatti et al. 1994):

$$R(\theta) = (1 + \tan^2\theta)\frac{\Delta Z_p}{2Z_p} - 8\left(\frac{V_s}{V_p}\right)^2 \sin^2\theta \frac{\Delta Z_s}{2Z_s} - \left[\frac{1}{2} \tan^2\theta - 2\left(\frac{V_s}{V_p}\right)^2 \sin^2\theta\right] \frac{\Delta\rho}{\rho} \quad (10)$$

After the P, S reflectivity's have been extracted; one can easily obtain the  $Z_p$  and  $Z_s$  through inversion. Finally, from equations 7 and 8 the transformation for  $\lambda\rho$  and  $\mu\rho$  is possible.

### 3. METHODS

The methodology adopted here is an integrated approach involving AVO modeling and seismic inversion. It is illustrated in figure 1.



Figure 2: Well log suite showing some transformed Logs with delineated gas sand (in black rectangle).

Table 1 shows the justification and power of the method in petrophysical analysis compared with other traditional and standard methods.

Table 1: Sensitivity Analysis of Various Rock Property Values at The Mapped Interface.						
	$V_p/V_s$	$(V_p/V_s)^2$	$\lambda+2\mu$	$\lambda$	$\mu$	$\lambda/\mu$
% Gas	1.94	3.75	23.47	9.30	7.09	1.38
% Shale	2.08	4.37	24.03	12.14	5.90	2.37
Average Change	6.73	14.2	2.3	23.4	16.8	41.8

In comparing columns 4, we notice the effect of decreasing  $\lambda$  (incompressibility) as a direct response of the gas porosity which in column 5 there is almost complete inverse by a rise in  $\mu$  (rigidity) while switching from capping shale to gas sand. However, it can be seen that by extracting the fluid term,  $\lambda$  and combing it into  $\lambda/\mu$  ratio, the average

changes of 23.4% for  $\lambda$  and 41.8% for  $\lambda/\mu$  are by far the most sensitive to variations in rock properties going from shale to gas sand. The conventional,  $V_p/V_s$  and  $(V_p/V_s)^2$  of 6.73% and 14.2% respectively are far less sensitive.

In performing AVO analysis, it is expected that crossplotting of these rock attributes be performed to separate the anomalous gas zone from the background trend. Figures 3 and 4 compare the crossplots of both the  $Z_p$ ,  $Z_s$  to  $\lambda\rho$ ,  $\mu\rho$  with the later been a better discriminator in isolating the gas zones. The  $I_p$ ,  $I_s$  plot (figure 3a) show a linear relationship (Castagna's mudrock line) with shale having the lowest values on both axes. Figure 4a presents a contrasting feature with the best gas sand cluster at the lowest  $\lambda\rho$  axis. This obvious enhanced effect of the  $\lambda\rho$ ,  $\mu\rho$  crossplot when compared to the  $Z_p$ ,  $Z_s$  crossplot is due to the fact that the axes are orthogonal with regard to Lamé parameters. Furthermore, from the vertical attribute (cross sections) of the generated crossplots, it is observed in 3b that the thin shale cap in between the gas zone was not discriminated as compared to 4b where it was easily mapped.

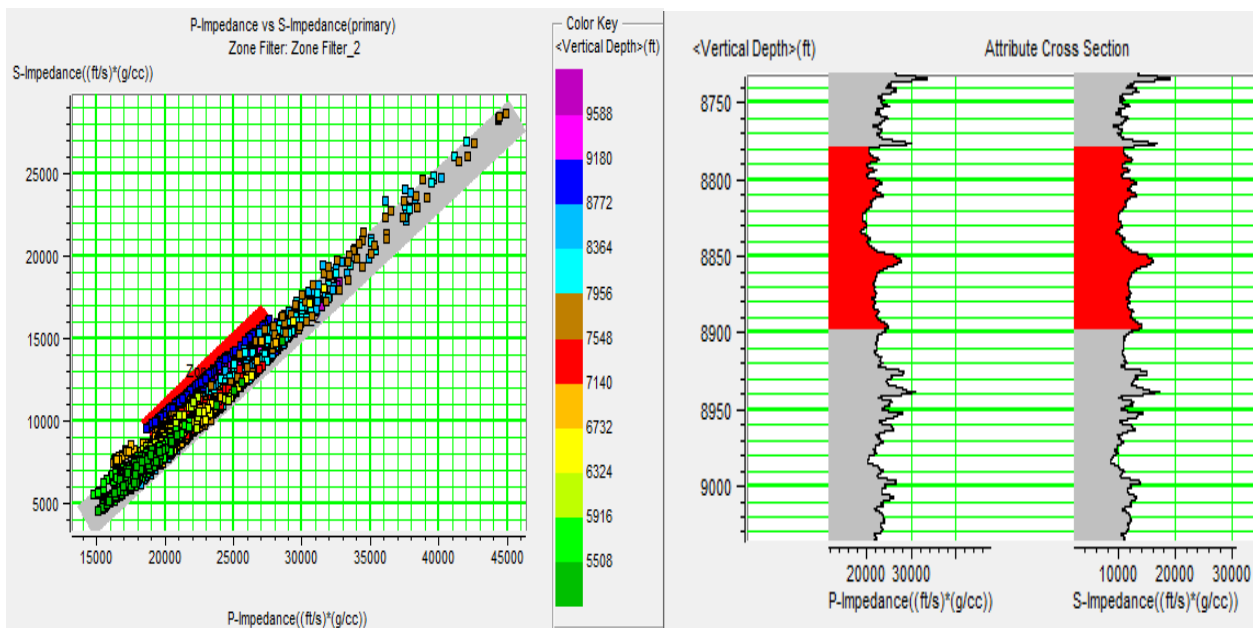


Figure 3: a)  $Z_p$ ,  $Z_s$  crossplot showing mapped zones; b)  $Z_p$ ,  $Z_s$  cross section display showing mapped zones

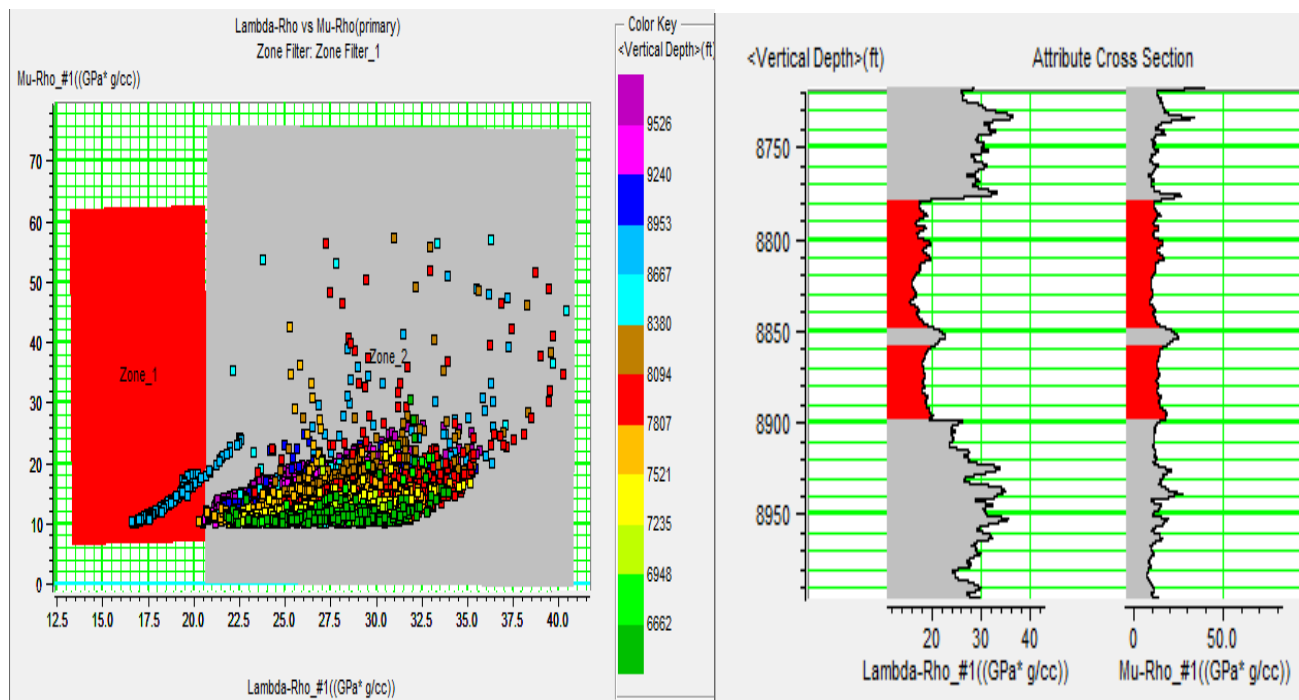


Figure 4: a)  $\lambda\rho$ ,  $\mu\rho$  crossplot showing mapped zones; b)  $\lambda\rho$ ,  $\mu\rho$  cross section display showing mapped zones

To further establish our interpretation, the  $\lambda\rho$ ,  $\mu\rho$  crossplot was generated as a function of various rock properties as colour indicators (figures 5-8). The mapped gas showed a high porosity value of about 40% which is

excellent for gas reservoirs (figure 5). This is further confirmed by the very low density (figure 6), very low water saturation values (figure 7) and low gamma ray values (figure 8).

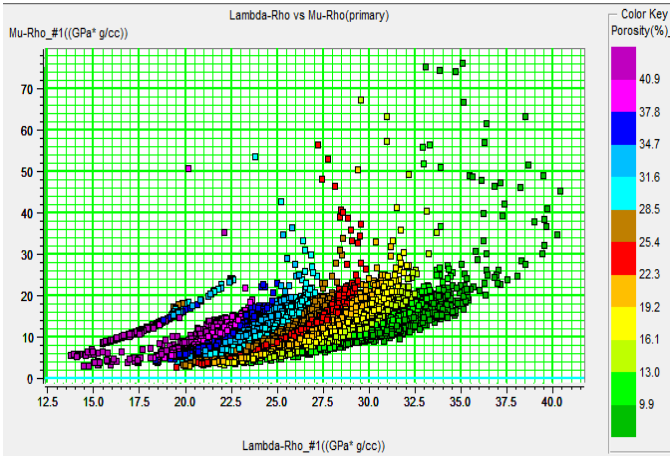


Figure 5:  $\lambda\rho$ ,  $\mu\rho$  crossplot, colour-coded to porosity.

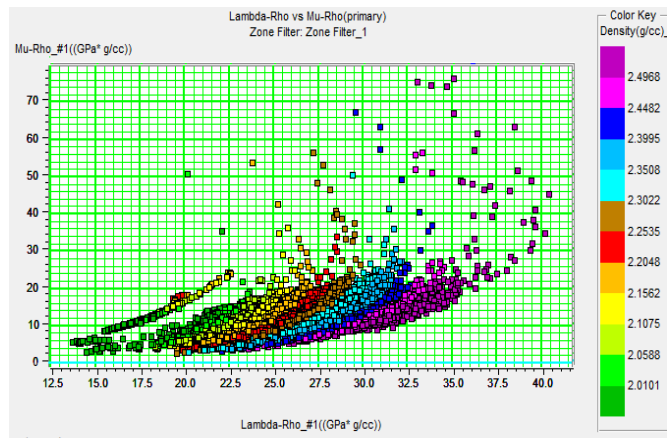


Figure 6:  $\lambda\rho$ ,  $\mu\rho$  crossplot, colour-coded to density.

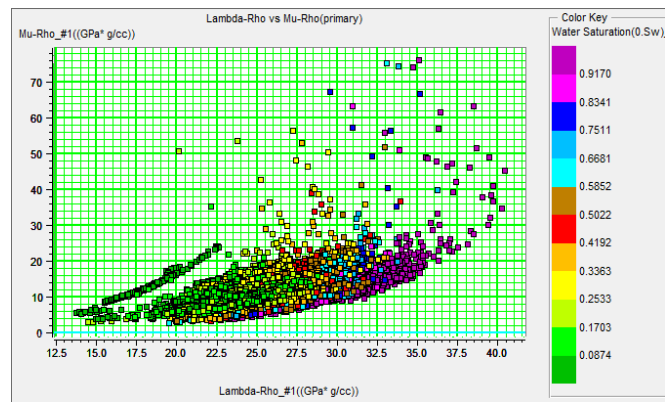


Figure 7:  $\lambda\rho$ ,  $\mu\rho$  crossplot, colour-coded to water saturation.

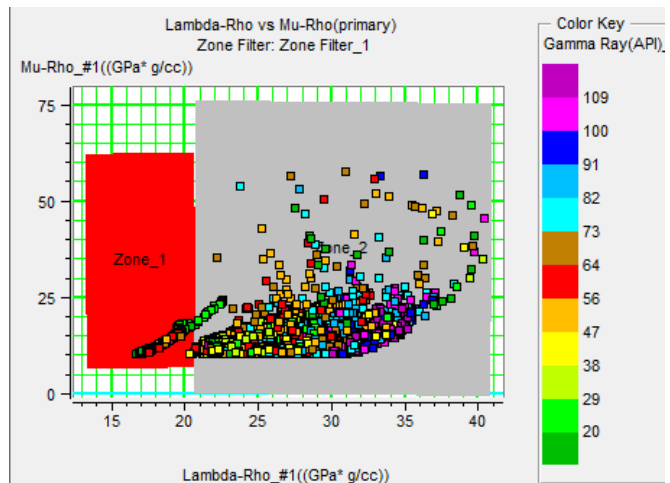


Figure 8:  $\lambda\rho$ ,  $\mu\rho$  crossplot, colour-coded to gamma ray.

It can be observed in figure 9 that the gas filled sands occupy lower  $\lambda\rho$  and  $\frac{\lambda}{\mu}$  values with the mapped sand identified to have a ratio less than 1 on the  $\frac{\lambda}{\mu}$  axis.

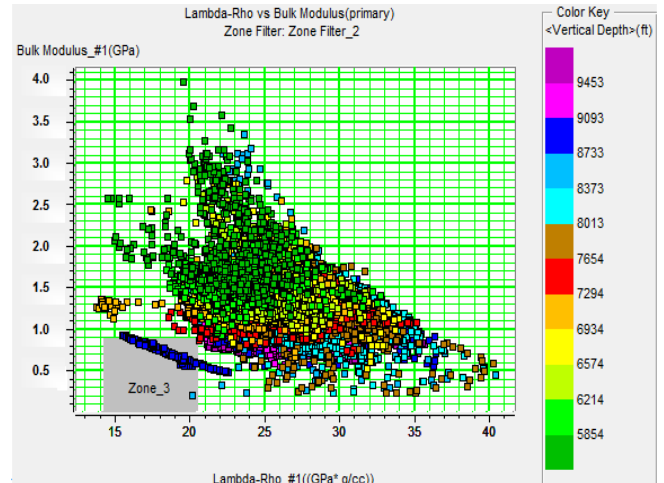


Figure 9:  $\lambda\rho$ ,  $\frac{\lambda}{\mu}$  crossplot showing mapped zone.

The results from wells were verified by the inverted seismic volume. Figure 10 shows the  $\lambda\rho$  seismic volume which isolate the gas zone as having low values that corresponds also with low values from the inserted  $\lambda\rho$  log. Figure 11 shows an improved discriminating power of this approach when the mapped zones as interpreted from the well were inserted. The gas zone is clearly seen on the time window which matches the well at depth. Taking amplitude slices that corresponds with the predicted well location at depth, it is observed that the mapped gas sand has low  $\lambda\rho$  (figure 12), moderate to high  $\mu\rho$  (figure 13) and low  $\frac{\lambda}{\mu}$  (figure 14). Using similar capture technique as applied to mapped gas sand, a possible prospect away from the well location was identified as an exploration interest (figure 15).

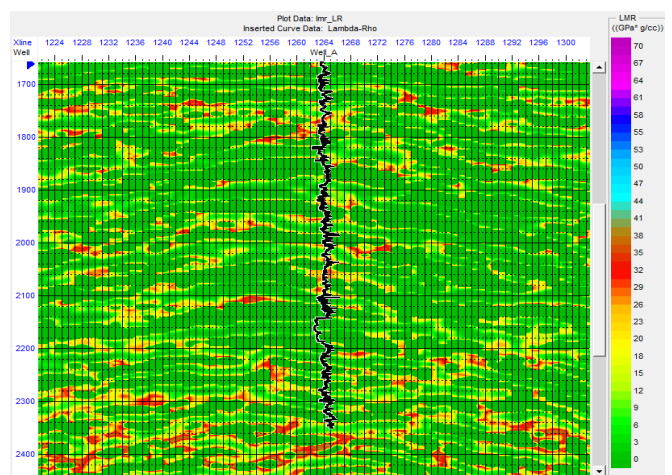


Figure 10:  $\lambda\rho$  volume with inserted  $\lambda\rho$  log showing low values at the mapped log dept.

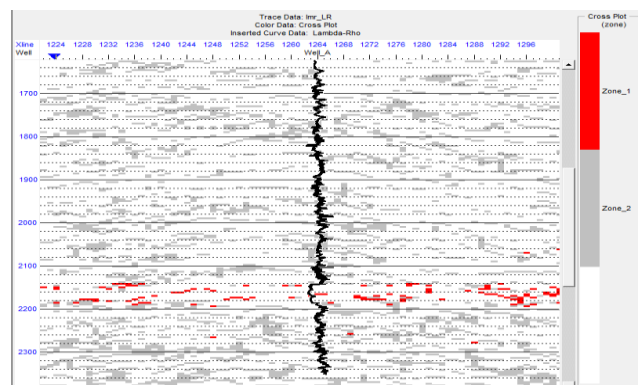


Figure 11:  $\lambda\rho$  volume with zones inserted.

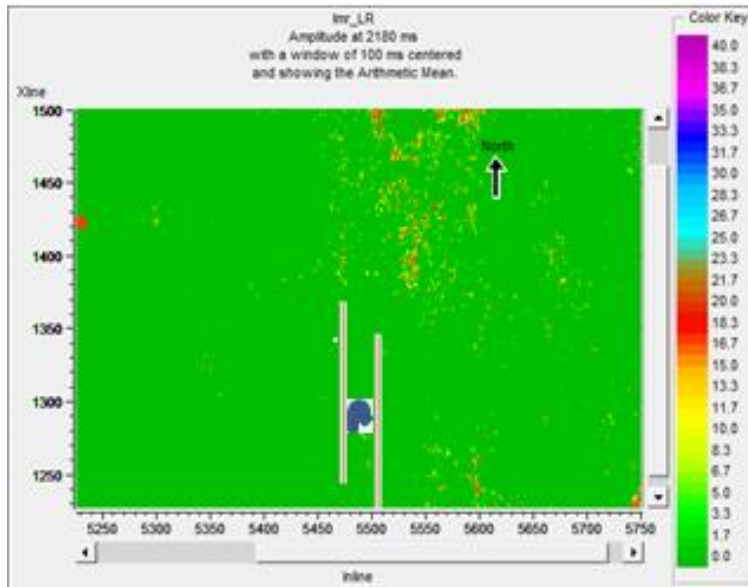


Figure 12: Amplitude slice of  $\lambda\rho$ . Lower values at well location ( ) confirms gas presence

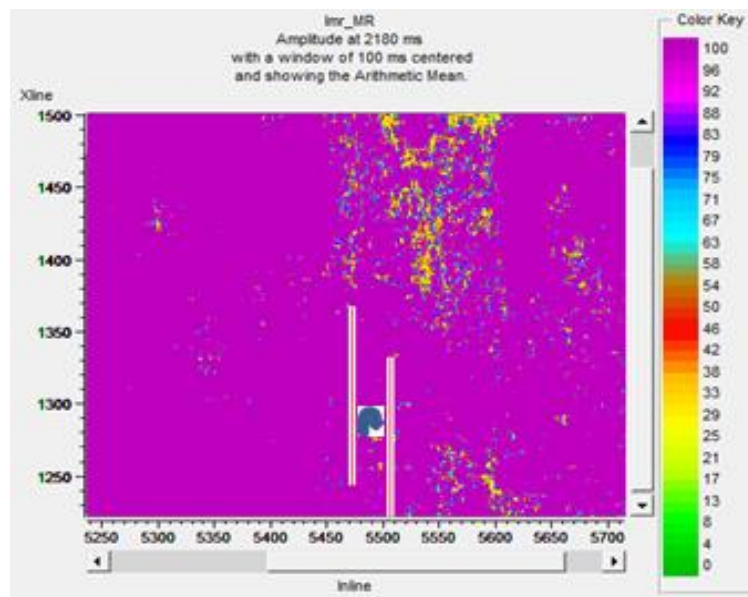


Figure 13: Amplitude slice of  $\mu\rho$ . Higher values at well location ( ) confirms gas presence.

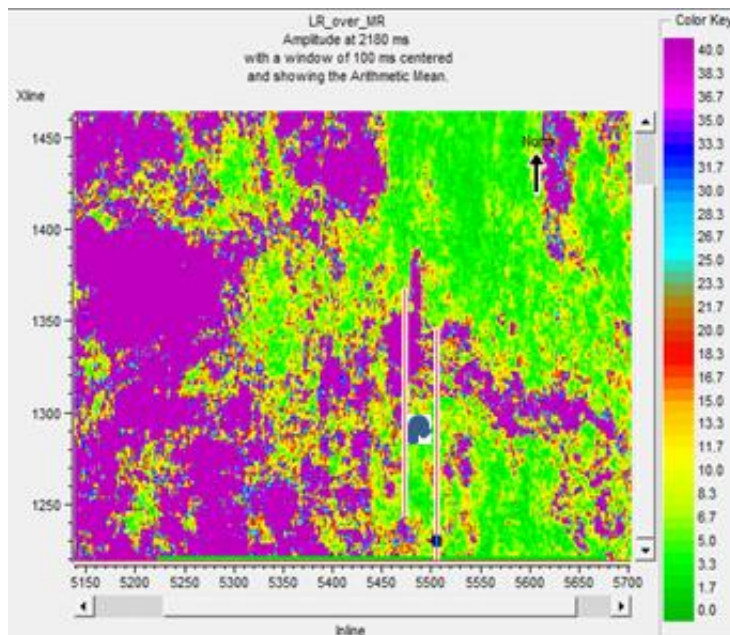
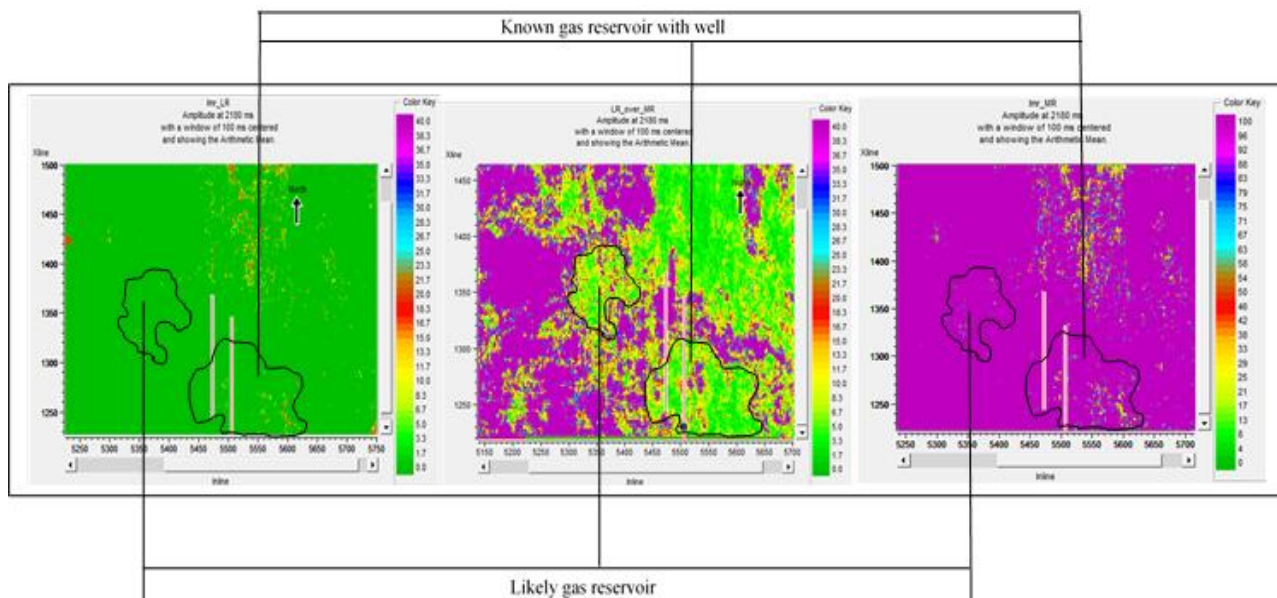


Figure 14: Amplitude slice of  $\frac{\lambda}{\mu}$ . Lower values at well location confirms gas presence



**Figure 15:** Amplitude slices of  $\lambda\rho$ ,  $\mu\rho$  and  $\frac{\lambda}{\mu}$  showing mapped gas sand at well location and a possible exploration target away from well.

## 5. CONCLUSION

It has been shown that better identification of reservoir zones is possible by the enhanced AVO method which showed sensitivity to pore fluids as well as lithology variations represented by fundamental changes in Lamé petrophysical parameters as opposed to the conventional parameters of seismic velocities. Moreover, from our case study the attributes  $\lambda\rho$  and  $\frac{\lambda}{\mu}$  were the most sensitive. The results show that moderate to high values of  $\mu\rho$  were indicative of clean sands and lower values of  $\lambda\rho$  and  $\frac{\lambda}{\mu}$  (<1) correlated well with areas containing gas. The inverted seismic volume validated the results from wells with the plots better aligned towards the lambda-rho axis thus justifying lambda-rho a better lithology discrimination tool. The good correlation of the inversion volumes with those of rock physics analysis observed at the wells provided confidence in our interpretation of a prospect away from the well thereby leading to discovery of another potential field in the region. The foregoing has confirmed that this approach can be used with confidence in delineating bypassed hydrocarbons in mature fields within the Niger Delta basin and thereby revive or increase production from such fields as well as mitigate the risk involved in finding hydrocarbons.

## ACKNOWLEDGEMENT

The authors are thankful to the Shell Petroleum Development Company (SPDC) of Nigeria for providing the dataset used.

## CONFLICT OF INTEREST

On behalf of all the co-authors, the corresponding author states that there is no conflict of interest.

## REFERENCES

Castagna, J.P., 1993a. Petrophysical imaging using AVO. TLE.

Castagna, J.P., Batzle, M.L., and Eastwood, R.L., 1985. Relationships between compressional-wave and shear-wave velocities in clastic silicate rocks. *Geophysics*, 50, Pp. 571-581.

Dewar, J., Downton, J., 2002. Getting unlost and staying found – a practical framework for interpreting elastic parameters.

Expanded Abstract CSEG Annual Conference.

Ekwe, A.C., Onuoha, K.M., and Osayande, N., 2012. Fluid and Lithology Discrimination Using Rock Physics Modelling and LambdaMuRho Inversion: An Example from Onshore Niger Delta, Nigeria.

Fatti, J.L., Smith, G.C., Vail, P.J., Strauss, P.J., Levitt, P.R., 1994. Detection of gas in sandstone reservoirs using AVO analysis: A 3D seismic case history using the Geostack technique. *Geophysics*, 59, Pp. 1362-1376.

Gassmann, F., 1951. Elastic waves through a packing of spheres. *Geophysics*, 16, Pp. 673-685.

Goodway, W., 2001. AVO and Lamé constants for rock parameterization and fluid detection. *Recorder*, 26, Pp. 39-60.

Goodway, W., Chen, T., and Downton, J., 1999. Rock parameterization & AVO fluid detection using Lamé petrophysical factors;  $\lambda$ ,  $\mu$  and  $\lambda\rho$ ,  $\mu\rho$ . 61<sup>st</sup> EAEG meeting, Expanded Abstracts, Pp. 6-51.

Nanda, N.C., 2016. *Seismic Data Interpretation and Evaluation for Hydrocarbon Exploration and Production: A Practitioner's Guide*. Springer International Publishing, Switzerland. 978-3-319-26491-2, Pp. 103-113.

Ohakwere-Eze, M., Igboekwe, M., Chukwu, G., 2018. Petrophysical evaluation and lithology delineation using cross-plots analysis from some onshore wells in the Nigerian-delta, West Africa. *International Journal of Advanced Geosciences*, 6 (1), Pp. 99-107.

Ostrander, W.J., 1984. Planewave reflection coefficients for gas sands at nonnormal angles of incidence. *Geophysics*, 49, Pp. 1637-1648.

Perez, M.A., Tonn, R., 2010. Reservoir Modelling and Interpretation with Lamé's parameters: A Grand Banks Case Study.

